Scientific Reports

https://doi.org/10.1038/s41598-026-36940-1

Article in Press

Orbitrap Astral–based proteome and phosphoproteome analysis identifies candidate proteins associated with the phosphatidate phosphatase MoPah1 in *Magnaporthe oryzae*

Received: 12 June 2025

Accepted: 18 January 2026

Published online: 02 February 2026

Cite this article as: Zhao J., Yang L., Shi X. *et al.* Orbitrap Astral–based proteome and phosphoproteome analysis identifies candidate proteins associated with the phosphatidate phosphatase MoPah1 in *Magnaporthe oryzae*. *Sci Rep* (2026). https://doi.org/10.1038/s41598-026-36940-1

Juan Zhao, Lili Yang, Xinyi Shi, Xinmei Zou, Bo Liu, Yong Wu, Chengming Zhang & Lan Xiang

We are providing an unedited version of this manuscript to give early access to its findings. Before final publication, the manuscript will undergo further editing. Please note there may be errors present which affect the content, and all legal disclaimers apply.

If this paper is publishing under a Transparent Peer Review model then Peer Review reports will publish with the final article.

ARTICLE IN PRESS

© The Author(s) 2026. **Open Access** This article is licensed under a Creative Commons Attribution-NonCommercial-NoDerivatives 4.0 International License, which permits any non-commercial use, sharing, distribution and reproduction in any medium or format, as long as you give appropriate credit to the original author(s) and the source, provide a link to the Creative Commons licence, and indicate if you modified the licensed material. You do not have permission under this licence to share adapted material derived from this article or parts of it. The images or other third party material in this article are included in the article's Creative Commons licence, unless indicated otherwise in a credit line to the material. If material is not included in the article's Creative Commons licence and your intended use is not permitted by statutory regulation or exceeds the permitted use, you will need to obtain permission directly from the copyright holder. To view a copy of this licence, visit http://creativecommons.org/licenses/by-nc-nd/4.0/.

ARTICLE IN PRESS

Orbitrap Astral–based proteome and phosphoproteome analysis identifies candidate proteins associated with the phosphatidate phosphatase MoPah1 in *Magnaporthe oryzae*

Juan Zhao[1,*], Lili Yang[2], Xinyi Shi[1], Xinmei Zou[1], Bo Liu[1], Yong Wu[1], Chengming Zhang[1], Lan Xiang[1]

[1] College of Chemistry and Life Sciences, Sichuan Provincial Key Laboratory for Development and Utilization of Characteristic Horticultural Biological Resources, Chengdu Normal University, Chengdu 611130, China

[2] Novogene Corporation Incorporated Company, Beijing 100000, China

* **Corresponding**: E-mail: zhaojuan201809@163.com

ARTICLE IN PRESS

ARTICLE IN PRESS

ABSTRACT

Background

Previous studies have shown that the phosphatidate phosphatase MoPah1 plays a critical role in *Magnaporthe oryzae* development and pathogenicity. The gene deletion mutant exhibits reduced virulence on rice leaves; however, the MoPah1 regulatory network remains unclear.

Result

In this study, we applied a quantitative data-independent acquisition approach using the Orbitrap Astral instrument to analyze the gene deletion mutant. We identified 6,799 proteins and 15,682 phosphorylation sites in *M. oryzae*, with differentially abundant proteins primarily enriched in metabolic and autophagy pathways. Integrating phosphoproteomic and proteomic analyses, we found 72 overlapping proteins. Additionally, we employed glutathione S-transferase pull-down and yeast two-hybrid assays to screen and verify MoPah1-interacting proteins, identifying Pmk1.

Conclusions

Our findings reveal candidate proteins in the MoPah1 regulatory network and the interaction between MoPah1 and Pmk1 in *M. oryzae*.

Keywords: *Magnaporthe oryzae*; phosphatidate phosphatase; proteomic; phosphoproteomics

ARTICLE IN PRESS

ARTICLE IN PRESS

INTRODUCTION

Phosphatidic acid (PA) is not only a key component of the cell membrane but also a signaling molecule involved in development and lipid metabolism [1]. In many organisms, cellular PA levels play a critical role in various biological processes, including lipid droplet biosynthesis and phospholipid metabolism, both of which are essential for cell development [2, 3]. In eukaryotic cells, phosphatidate phosphatases (PAPs) catalyze the conversion of PA into diacylglycerol, a central molecule in phospholipid and triacylglycerol biosynthesis, while also regulating lipid-signaling pathways [4, 5]. Previous studies have shown that the PAP of *Magnaporthe oryzae*, MoPah1, the pathogen responsible for rice blast, is localized in the cytoplasm, and its loss of function leads to increased PA levels [6-8].

Magnaporthe oryzae, a typical filamentous ascomycete, relies on specialized infection structures called appressoria to generate turgor pressure for plant infection [9-11]. During appressorium formation, glycogen stored in conidia is rapidly utilized, highlighting the critical role of lipid metabolism in this process [12, 13]. Beyond MoPah1, several lipid metabolism–related mutants exhibit defects in appressorium formation and pathogenicity [12, 14]. Mutations in the glycogen metabolic proteins AGL1 and GPH1 and the cytosolic glycerol-3-phosphate dehydrogenase proteins GPD1 and GPD2 reduce virulence in rice [15, 16]. Therefore, studying the MoPah1-centered regulatory network is crucial for understanding the relationship between lipid metabolism and pathogenesis.

Several studies have analyzed the *M. oryzae* proteome in relation to pathogenicity. The tandem mass tag (TMT)-based quantitative proteomics approach has been widely used for such analyses [17, 18]. However, accurate proteomic and phosphoproteomics studies of *M. oryzae* using a quantitative data-independent

ARTICLE IN PRESS

acquisition (DIA) approach remain limited. In recent years, DIA mass spectrometry (MS) has demonstrated greater reproducibility and sensitivity compared with traditional data-dependent acquisition methods [19, 20]. Advances in proteomic instrumentation have led to the development of Thermo's next-generation tandem mass spectrometer, the Astral multi-reflection analyzer, featuring a total secondary flight path exceeding 30 m [21]. Hence, it is necessary to employ the DIA approach to explore the protein interaction network of MoPah1.

In this study, we employed a DIA approach to analyze the proteomes and phosphoproteomes of *M. oryzae* wild-type (WT) and the MoPah1 knockout mutant mycelium, in which the PAP gene was knocked out, resulting in lower PA content than that in the WT. The mutant lacks conidia for appressorium formation, but its hyphae can still form appressorium-like structures capable of plant infection. Therefore, mycelium samples were used for total protein extraction, with three independent biological replicates per genotype. Proteomics and phosphoproteomics confirmed the absence of MoPah1 synthesized in the mutant, consistent with previous reports. Given the importance of MoPah1 in *M. oryzae*, we identified and analyzed MoPah1-interacting proteins using a glutathione S-transferase (GST) pull-down assay and MS. Our findings identify candidate proteins associated with the MoPah1 network and reveal the protein interaction relationship between MoPah1 and Pmk1.

ARTICLE IN PRESS

Materials and methods

Experimental Design

We employed a DIA approach to analyze the proteomes and phosphoproteomes of *M. oryzae* wild-type (WT) and the MoPah1 deletion mutant (M21) mycelium, in which

ARTICLE IN PRESS

the PAP gene was knocked out, resulting in lower PA content than that in the WT. The mutant lacks conidia for appressorium formation, but its hyphae can still form appressorium-like structures capable of plant infection. Therefore, mycelium samples were used for total protein extraction, with three independent biological replicates per genotype. The workflow used to analyze protein abundance and phosphorylation changes caused by the MoPah1 mutation is shown in **Figure 1**. Proteomics and phosphoproteomics confirmed the absence of MoPah1 expression in the mutant, consistent with previous reports. Given the importance of MoPah1 in *M. oryzae*, we identified and analyzed MoPah1-interacting proteins using a glutathione S-transferase (GST) pull-down assay and MS.

Strains and culture conditions

The *M. oryzae* WT strain P131 and mutant (M21) were used for proteome and phosphoproteome analyses [22]. Strains were cultured in liquid minimal medium at 28°C with shaking at 120 rpm for 4 days. Mycelia were harvested and flash-frozen in liquid nitrogen for proteomics and GST pull-down experiments.

Total protein extraction

Total protein was extracted from frozen mycelia using SDT lysis buffer [100 mM NaCl and 1% DL-Dithiothreitol (Sigma)]. The lysate was ultrasonicated, incubated in an ice bath, and centrifuged at 4°C. The supernatant was incubated with iodoacetamide at room temperature in the dark for 1 h. Samples were then mixed with four volumes of precooled acetone and incubated at −20°C for at least 2 h. After centrifugation, the precipitate was collected, washed with cold acetone, and dissolved in dissolution buffer (8 M urea and 100 mM triethylammonium bicarbonate at pH

ARTICLE IN PRESS

8.5). Protein quality was assessed using a Bradford protein quantification kit according to the manufacturer's instructions (Takara, Japan).

Trypsin treatment

Trypsin treatment followed a previously described protocol [23]. Trypsin and 100 mM TEAB buffer were added to protein samples and incubated at 37°C for 4 h, followed by overnight digestion with trypsin and $CaCl_2$. Formic acid was added to adjust the pH below 3, and the supernatant was collected after centrifugation. Samples were loaded onto a C18 desalting column, and eluents were collected and lyophilized.

Liquid chromatography-MS/MS analysis in DIA mode

Lyophilized samples were dissolved in 10 μL of solution A (100% water and 0.1% formic acid) and centrifuged, and the supernatant was used for liquid chromatography (LC) analysis. A Vanquish Neo upgraded ultra-high-performance LC (UHPLC) system was used with a C18 precolumn (174500, 5 mm × 300 μm, 5 μm; Thermo) heated to 50°C in a column oven and a C18 analytical column (ES906, PepMap™ Neo UHPLC 150 μm × 15 cm, 2 μm; Thermo). Elution conditions for proteome and phosphoproteome analysis are shown in **Tables 1** and **2**, respectively. A Thermo Orbitrap Astral mass spectrometer was used in DIA mode (m/z 380–980 first-stage scanning range, 240,000 MS resolution, 500% AGC, 2-Th parent ion window size, 300 DIA windows, 25% NCE, m/z 150–2000 secondary-stage scanning range, 80,000 sub-ion resolution, and 3-ms injection time). An Easy-Spray ion source (1.9 kV and 290°C) was employed in these analyses.

Table 1. Liquid chromatography elution gradient table for proteome

Time	flow rate (nL/min)	mobile phase A (%)	mobile phase B (%)

ARTICLE IN PRESS

0	2.5	96	4
0.2	2.0	96	4
0.3	1.5	96	4
0.4	0.8	92	8
0.7	0.8	92	8
13.7	0.8	77.5	22.5
20.6	0.8	65	35
21	2	45	55
21.5	2.5	1	99
23.8	2.5	1	99

Table 2. Liquid chromatography elution gradient table for phosphoproteome

Time	flow rate (nL/min)	mobile phase A (%)	mobile phase B (%)
0	2.5	96	4
0.2	1.3	96	4
0.3	0.8	92	8
0.5	0.8	92	8
14.2	0.8	77.5	22.5
21.1	0.8	65	35
21.5	2.5	45	55
21.5	Column Wash		
21.9	2.5	1	99

ARTICLE IN PRESS

ARTICLE IN PRESS

22.6	2.5	1	99
22.6	Stop Run		

Proteomic analysis

Raw data were searched and analyzed using DIA-NN library search software (1.6.0) (https://github.com/vdemichev/diann) against the Uniport database (https://www.uniprot.org/) [24]. Mass tolerances were set to 10 ppm for precursor ions and 0.02 Da for fragment ions. To improve data quality, only peptide spectrum matches with a confidence level of ≥99% were retained. False discovery rate (FDR) validation was used to remove peptides and proteins with an FDR >1%.

Phosphoproteomic analysis

Raw phosphoproteomic data were analyzed using Spectronaut 20 software (https://biognosys.com/software/spectronaut/) with the Uniport database. As in proteomic analysis, only peptide spectrum matches with a confidence level ≥99% were retained, and FDR validation removed peptides and proteins with an FDR >1%. Retention time correction was performed using iRT standards, and the precursor ion Q value cutoff value was set to 0.01.

ARTICLE IN PRESS

Functional analysis

Gene Ontology (GO) and Kyoto Encyclopedia of Genes and Genomes databases were used to analyze protein families and pathways [25-27]. Protein interactions were predicted using STRING DB (http://STRING.embl.de/) [28]. Phosphorylation site motif enrichment analysis was performed using the motif-x algorithm, with seven individual residues flanking the central residue [29].

GST pull-down and MS

GST and MoPah1–GST fusion proteins were purified as previously described [30]. The full-length MoPah1 was inserted into the pGEX-6p-1 vector using a one-step

ARTICLE IN PRESS

cloning kit (Vazyme, China), and the recombinant plasmid was introduced into *E. coli* BL21(DE3) cells. MoPah1-GST fusion protein expression was induced with 1.0 mM isopropyl β-D-thiogalactoside (IPTG) in LB medium at 16°C for 12 hours. Bacterial cells were harvested by centrifugation, resuspended in phosphate-buffered saline (PBS) buffer, and lysed by sonication. Following centrifugation, the supernatant was purified using GST-affinity chromatography with GST NUPharose 4B (Nuptec, China). After washing with PBS buffer, the target protein was eluted with elution buffer (50 mM Tris-HCl, 10 mM reduced glutathione, pH 8.0).

Briefly, beads carrying GST or MoPah1–GST were incubated with total *M. oryzae* protein at 4°C for 2 h after washing the protein complexes three times with PBS buffer; they were incubated with *M. oryzae* total protein. The beads were then washed five times with PBS buffer and boiled in loading buffer. Proteins were detected using western blotting and MS. Data analysis was performed using UniProt [31].

Yeast two-hybrid assays

For yeast two-hybrid assays, the MoPah1 open reading frame was cloned into the pGBKT7 plasmid using primers PAH1-HF and PAH1-HR. The Pmk1-AD plasmid established in previous studies [32, 33] was used. MoPah1 and Pmk1 constructs were cotransformed into the *Saccharomyces cerevisiae* AH109 strain. Transformants were grown on SD-Leu/Trp and SD-Leu/Trp/His/Ade plates with X-Gal.

Statistical analysis

Differential protein and phosphorylation site quantification was statistically analyzed using the *t*-test. Proteins and phosphorylation sites were considered differentially abundant if $P < 0.05$ and fold change < 0.5 (downregulated) or > 2.0 (upregulated).

RESULTS

ARTICLE IN PRESS

Proteome and phosphoproteome profiling of M. oryzae using quantitative DIA analysis

Principal component analysis revealed a significant difference between the WT and M21 mutant samples, confirming the reliability of our proteomic and phosphoproteomic datasets **(Supplemental Figure)**. In total, 6,799 proteins were identified in the non-modified proteome analysis **(Supplemental Table 1)**. For quantitative analysis, 6,670 proteins were identified, with 539 significantly differentially abundant proteins (DAP) observed in the M21 mutant **(Figure 2A** and **Supplemental Table 2)**. The results showed that 329 proteins decreased and 210 proteins increased in the mutant **(Figure 2B)**.

For phosphoproteome analysis, 16,296 phosphorylation sites were quantified across 3,539 proteins using Spectronaut software (Precursor Q-value cutoff: 0.01; **Figure 2C** and **Supplemental Table 3**). After normalization with protein quantitation, 15,682 phosphorylation sites on 2,349 proteins were identified. In total, 3,770 phosphorylation sites on 1,092 proteins met the criteria for DAP phosphoproteins (DAPPs; **Supplemental Table 4)**, which were identical to those for DAPPs. Among these, 1,788 and 1,982 phosphorylation sites showed decreased and increased levels in the mutant, respectively **(Figure 2D)**. These findings demonstrate that the loss of MoPah1 function led to widespread alterations in the proteome and phosphoproteome.

Using the latest Orbitrap Astral mass spectrometer, our DIA approach provided high-resolution proteomic data for *M. oryzae* **(Figure 2A, B)** [34, 35]. Notably, MS-based large-scale profiling of protein composition and dynamic regulation has become a key tool in proteomic analysis [36]. Compared with previous proteomic datasets [37], our study offers improved identification and quantification accuracy, supporting

ARTICLE IN PRESS

in-depth protein network analysis in *M. oryzae*.

Identification and characterization of DAPs and phosphoproteins in the mutant

As a protein phosphatase, MoPah1 plays a crucial role in protein phosphorylation, regulating numerous cellular processes [38]. Additionally, protein function is influenced by subcellular localization in eukaryotes [39]. To determine the compartmentalization of DAPs and DAPPs, we used the Cell-mPLOC 2.0 web server for subcellular protein localization prediction [40]. The analysis revealed distinct distributions: 39 DAPs were primarily cytoplasmic **(Supplemental Table 5)**, whereas 203 DAPPs were mainly nuclear **(Figure 3A, B; Supplemental Table 6)**, suggesting that MoPah1 phosphorylation occurs predominantly in the nucleus. Furthermore, we identified 72 proteins with significant changes in both the phosphoproteome and proteome, indicating that they are major targets of MoPah1-mediated regulation **(Figure 3C** and **Supplemental Table 7)**. Among them, three proteins exhibited opposing patterns of phosphorylation and protein synthesis, suggesting that phosphorylation may influence their turnover.

To investigate biological processes affected by the MoPah1 mutation, we performed GO enrichment analysis. DAPs and DAPPs were distributed across 35 biological processes **(Figure 4A, B)**. Given the alterations in lipid metabolism in the mutant, both DAPs and DAPPs were enriched in glycerophospholipid metabolism signaling. These results suggest that the MoPah1 mutation triggers lipid metabolism and autophagy pathways.

Phosphoproteomic analysis of protein kinases and phosphorylated motifs

To further explore posttranslational modifications, we analyzed protein kinases, which regulate diverse biological processes by catalyzing phosphorylation. Group-based Prediction System 6.0 was used to identify protein kinases in the mutant [41]. In the

ARTICLE IN PRESS

kinase-substrate prediction analysis, CMGC/MAPK family kinases were enriched and showed the highest prediction scores for potential regulation by/phosphorylation by MoPah1 **(Supplemental Table 8)**. Given that phosphorylation requires specific amino acid sequence motifs, we performed motif analysis (peptides > 20, *P*-value cutoff = 1e-6) using the method established by Wagih [42]. Results showed that serine motifs were the predominant phosphorylation sites in the mutant, with an increased number compared to the WT **(Supplemental Table 9)**.

Protein–protein interactions

To explore interactions between DAPs and DAPPs, we used STRING-DB to construct functional association networks, focusing on DAPs **(Figure 5A)** and DAPPs **(Figure 5B)** in the mutant. The networks showed that DAPs and DAPPs were involved in lipid and amino acid metabolism. Compared with DAPs, DAPPs were more enriched in autophagy, endocytosis, cell cycle regulation, RNA transport, and ribosome-associated processes.

The GST pull-down assay, a widely used biochemical method for studying protein–protein interactions in *vitro* [43], was employed to further investigate MoPah1 interactions. In our previous study, we successfully expressed and purified a MoPah1-GST protein in *Escherichia coli* **(Figure 6A)**. In the present study, MoPah1-GST was used as a probe to identify interacting proteins. MS analysis identified 183 MoPah1-interacting proteins, enriched in protein-containing complexes, confirming MoPah1's role in the protein network **(Figure 6B** and **Supplemental Table 10)**. Additionally, the GST pull-down assays confirmed that MoPah1-GST interacted with Pmk1. Yeast two-hybrid assays further validated this interaction, as Pmk1-AD was found to interact with MoPah1-BD **(Figure 6C)**, suggesting that MoPah1 directly interacts with Pmk1.

ARTICLE IN PRESS

DISCUSSION

Phosphatidate phosphatases are critical enzymes in lipid metabolism and play a key role in fungal pathogenicity [44-46]. This study aimed to characterize the proteome and phosphoproteome of the mutant using a DIA approach with the Orbitrap Astral mass spectrometer, providing insights into candidate proteins associated with the MoPah1 regulatory network.

The DIA approach was chosen for its ability to provide accurate site localization and reproducible quantification of proteomic data **(Figure 2)** [21]. Traditionally, data-dependent acquisition (DDA) methods, such as iTRAQ/TMT, label-free, and SILAC, have been widely used for proteomic analysis [19, 20]. However, compared with DDA, the DIA approach offers higher-resolution proteomic data with improved sensitivity and reproducibility. With advances in MS technology, the next-generation tandem mass spectrometer developed by Thermo, which features the powerful Astral multi-reflection analyzer, has markedly enhanced proteomic analysis [21]. Therefore, this study represents the first report on *M. oryzae* using DIA-based proteomic and phosphoproteomic analysis with the Orbitrap Astral instrument, leading to the identification of a greater number of proteins and phosphorylation sites.

GO enrichment and protein–protein interaction analysis revealed that lipid metabolism and the autophagy pathway were extensively altered in the mutant, confirming findings from our previous studies **(Figures 4** and **5)** [8]. Furthermore, the present study demonstrated that the glycerophospholipid metabolic process is the primary lipid metabolism pathway affected in the mutant. Among the DAPs and DAPPs involved in glycerophospholipid metabolism, glycerol-3-phosphate o-acyltransferase 1 was identified, which is upstream of the *PAH1* gene and the primary

ARTICLE IN PRESS

supplier of diacylglycerols in yeast [47]. Additionally, the autophagy signaling pathway was mainly altered at the phosphoproteome level, with significant changes in the phosphorylation levels of proteins, such as autophagy-related protein ATG3, which has been reported to be regulated by PA levels in *Arabidopsis* [48]. These findings, reported here for the first time, provide insights into the MoPah1 regulatory network.

Consistent with our previous study, protein kinase and phosphorylated motif analysis further demonstrated that the MAPK signaling pathway was altered in the mutant. Additionally, three important mitogen-activated protein kinases (Mps1, Pmk1, and Osm1) of the MAPK signaling pathway, which are crucial for regulating cell wall integrity, appressorium-mediated host penetration, infectious hyphal growth, and osmotic stress responses, were implicated [49, 50]. The predicted phosphorylation sites mainly concentrated in Mps1, Pmk1, and Osm1, which aligns with our previous findings regarding the alterations of these protein kinases in the mutant. This suggests that these protein kinases are likely involved in phosphorylating MoPah1 (**Supplemental Table 8**) [51-53].

ARTICLE IN PRESS

Specifically, we observed that Pmk1 protein expression was decreased in the mutant, suggesting that MoPah1 is primarily involved in the Pmk1–MAPK signaling pathway [8], which is crucial for the control of appressorium formation, an essential step in fungal pathogenicity. Moreover, results from yeast two-hybrid assays and GST pull-down experiments further confirmed the interaction between MoPah1 and Pmk1, indicating that MoPah1 regulates pathogenicity through the Pmk1–MAPK pathway **(Figure 6)**. A prior study found that MoPah1 phosphorylation levels were markedly altered in the Pmk1 deletion mutant during appressorium phosphoproteomic analysis, in contrast to our findings from hyphal proteomics and phosphoproteomics [54]. This

ARTICLE IN PRESS

discrepancy may be attributed to differences in developmental stages during data collection, as Pmk1 mainly functions in the appressorium formation stage. However, Pmk1 phosphorylation was not changed in the MoPah1 deletion mutant (**Supplemental Table 4**). These results indicated that Pmk1 is likely an upstream regulator of MoPah1.

A limitation of this study is that hyphal samples may not have been the optimal choice; however, because the MoPah1 deletion mutant does not produce spores, we were limited to analyzing mycelial samples.

ACKNOWLEDGEMENTS

We acknowledge Novogene Corporation Incorporated Company support the proteomic analysis and Biorun Incorporated Company support for the protein screening.

FUNDING

This work was supported by the National Natural Science Foundation of China (No. 32402340) and the Natural Science Foundation of Sichuan, China (No. 2024NSFSC1320).

DATA AVAILABILITY

Our raw data of proteomics and phosphoproteomics have been deposited in the ProteomeXchange Consortium (https://proteomecentral.proteomexchange.org) via the iProX partner repository with the dataset identifiers PXD056310 and PXD062656, respectively.

REFERENCES

1. Young BP, Shin JJ, Orij R, Chao JT, Li SC, Guan XL, Khong A, Jan E, Wenk

ARTICLE IN PRESS

ARTICLE IN PRESS

MR, Prinz WA *et al*: **Phosphatidic acid is a pH biosensor that links membrane biogenesis to metabolism**. *Science* 2010, **329**(5995):1085-1088.

2. Fei W, Shui G, Zhang Y, Krahmer N, Ferguson C, Kapterian TS, Lin RC, Dawes IW, Brown AJ, Li P *et al*: **A role for phosphatidic acid in the formation of "supersized" lipid droplets**. *PLoS Genet* 2011, **7**(7):e1002201.

3. Athenstaedt K: **Phosphatidic acid biosynthesis in the model organism yeast Saccharomyces cerevisiae - a survey**. *Biochim Biophys Acta Mol Cell Biol Lipids* 2021, **1866**(6):158907.

4. Adeyo O, Horn PJ, Lee S, Binns DD, Chandrahas A, Chapman KD, Goodman JM: **The yeast lipin orthologue Pah1p is important for biogenesis of lipid droplets**. *J Cell Biol* 2011, **192**(6):1043-1055.

5. Carman GM, Han G-S: **Roles of phosphatidate phosphatase enzymes in lipid metabolism**. *Trends in Biochemical Sciences* 2006, **31**(12):694-699.

6. Meng S, Torto-Alalibo T, Chibucos MC, Tyler BM, Dean RA: **Common processes in pathogenesis by fungal and oomycete plant pathogens, described with Gene Ontology terms**. *BMC Microbiol* 2009, **9 Suppl 1**(Suppl 1):S7.

7. Fernandez J, Orth K: **Rise of a cereal killer: The biology of *magnaporthe oryzae* biotrophic growth**. *Trends Microbiol* 2018, **26**(7):582-597.

8. Zhao J, Sun P, Sun Q, Li R, Qin Z, Sha G, Zhou Y, Bi R, Zhang H, Zheng L *et al*: **The MoPah1 phosphatidate phosphatase is involved in lipid metabolism, development, and pathogenesis in Magnaporthe oryzae**. *Mol Plant Pathol*

ARTICLE IN PRESS

2022, **23**(5):720-732.

9. Kong LA, Li GT, Liu Y, Liu MG, Zhang SJ, Yang J, Zhou XY, Peng YL, Xu JR: **Differences between appressoria formed by germ tubes and appressorium-like structures developed by hyphal tips in *Magnaporthe oryzae***. *Fungal Genet Biol* 2013, **56**:33-41.

10. Wilson RA, Talbot NJ: **Under pressure: Investigating the biology of plant infection by *Magnaporthe oryzae***. *Nat Rev Microbiol* 2009, **7**(3):185-195.

11. Ryder LS, Talbot NJ: **Regulation of appressorium development in pathogenic fungi**. *Curr Opin Plant Biol* 2015, **26**:8-13.

12. Foster AJ, Ryder LS, Kershaw MJ, Talbot NJ: **The role of glycerol in the pathogenic lifestyle of the rice blast fungus *Magnaporthe oryzae***. *Environ Microbiol* 2017, **19**(3):1008-1016.

13. De Jong JC, McCormack BJ, Smirnoff N, Talbot NJ: **Glycerol generates turgor in rice blast**. *Nature* 1997, **389**(6648):244-245.

14. Fernandez J, Wright JD, Hartline D, Quispe CF, Madayiputhiya N, Wilson RA: **Principles of carbon catabolite repression in the rice blast fungus: Tps1, Nmr1-3, and a MATE-family pump regulate glucose metabolism during infection**. *PLoS Genet* 2012, **8**(5):e1002673.

15. Badaruddin M, Holcombe LJ, Wilson RA, Wang ZY, Kershaw MJ, Talbot NJ: **Glycogen metabolic genes are involved in trehalose-6-phosphate synthase-mediated regulation of pathogenicity by the rice blast fungus *Magnaporthe oryzae***. *PLoS Pathog* 2013, **9**(10):e1003604.

ARTICLE IN PRESS

ARTICLE IN PRESS

16. Shi Y, Wang H, Yan Y, Cao H, Liu X, Lin F, Lu J: **Glycerol-3-phosphate shuttle is involved in development and virulence in the rice blast fungus *Pyricularia oryzae***. *Front Plant Sci* 2018, **9**(687):687.

17. Chen X, Xu Q, Yue Y, Duan Y, Liu H, Chen X, Huang J, Zheng L: **Comparative oxidation proteomics analyses suggest redox regulation of cytosolic translation in rice leaves upon Magnaporthe oryzae infection**. *Plant Commun* 2023, **4**(3):100550.

18. Chen Y, Wu X, Chen C, Huang Q, Li C, Zhang X, Tan X, Zhang D, Liu Y: **Proteomics Analysis Reveals the Molecular Mechanism of MoPer1 Regulating the Development and Pathogenicity of Magnaporthe oryzae**. *Front Cell Infect Microbiol* 2022, **12**:926771.

19. Chen X, Sun Y, Zhang T, Shu L, Roepstorff P, Yang F: **Quantitative Proteomics Using Isobaric Labeling: A Practical Guide**. *Genomics Proteomics Bioinformatics* 2021, **19**(5):689-706.

20. Bichmann L, Gupta S, Röst H: **Data-Independent Acquisition Peptidomics**. *Methods Mol Biol* 2024, **2758**:77-88.

21. Dumas T, Martinez Pinna R, Lozano C, Radau S, Pible O, Grenga L, Armengaud J: **The astounding exhaustiveness and speed of the Astral mass analyzer for highly complex samples is a quantum leap in the functional analysis of microbiomes**. *Microbiome* 2024, **12**(1):46.

22. Zhao J, Sun P, Sun Q, Li R, Qin Z, Sha G, Zhou Y, Bi R, Zhang H, Zheng L *et al*: **The MoPah1 phosphatidate phosphatase is involved in lipid metabolism,**

ARTICLE IN PRESS

development, and pathogenesis in *Magnaporthe oryzae*. *Mol Plant Pathol* 2022.

23. Zhang H, Liu T, Zhang Z, Payne SH, Zhang B, McDermott JE, Zhou JY, Petyuk VA, Chen L, Ray D *et al*: **Integrated Proteogenomic Characterization of Human High-Grade Serous Ovarian Cancer**. *Cell* 2016, **166**(3):755-765.

24. Demichev V, Messner CB, Vernardis SI, Lilley KS, Ralser M: **DIA-NN: neural networks and interference correction enable deep proteome coverage in high throughput**. *Nature Methods* 2020, **17**(1):41-44.

25. Ashburner M, Ball CA, Blake JA, Botstein D, Butler H, Cherry JM, Davis AP, Dolinski K, Dwight SS, Eppig JT *et al*: **Gene ontology: tool for the unification of biology. The Gene Ontology Consortium**. *Nat Genet* 2000, **25**(1):25-29.

26. Kanehisa M, Goto S, Hattori M, Aoki-Kinoshita KF, Itoh M, Kawashima S, Katayama T, Araki M, Hirakawa M: **From genomics to chemical genomics: new developments in KEGG**. *Nucleic Acids Res* 2006, **34**(Database issue):D354-357.

27. Finn RD, Attwood TK, Babbitt PC, Bateman A, Bork P, Bridge AJ, Chang HY, Dosztányi Z, El-Gebali S, Fraser M *et al*: **InterPro in 2017-beyond protein family and domain annotations**. *Nucleic Acids Res* 2017, **45**(D1):D190-d199.

28. Franceschini A, Szklarczyk D, Frankild S, Kuhn M, Simonovic M, Roth A, Lin J, Minguez P, Bork P, von Mering C *et al*: **STRING v9.1: protein-protein interaction networks, with increased coverage and integration**. *Nucleic Acids Res* 2013, **41**(Database issue):D808-815.

ARTICLE IN PRESS

29. Kachuk C, Stephen K, Doucette A: **Comparison of sodium dodecyl sulfate depletion techniques for proteome analysis by mass spectrometry**. *J Chromatogr A* 2015, **1418**:158-166.

30. Vikis HG, Guan KL: **Glutathione-S-transferase-fusion based assays for studying protein-protein interactions**. *Methods Mol Biol* 2004, **261**:175-186.

31. Consortium U: **UniProt: the Universal Protein Knowledgebase in 2023**. *Nucleic Acids Res* 2023, **51**(D1):D523-d531.

32. Brückner A, Polge C, Lentze N, Auerbach D, Schlattner U: **Yeast two-hybrid, a powerful tool for systems biology**. *Int J Mol Sci* 2009, **10**(6):2763-2788.

33. Dube DH, Li B, Greenblatt EJ, Nimer S, Raymond AK, Kohler JJ: **A two-hybrid assay to study protein interactions within the secretory pathway**. *PLoS One* 2010, **5**(12):e15648.

34. Liu N, Qi L, Huang M, Chen D, Yin C, Zhang Y, Wang X, Yuan G, Wang RJ, Yang J *et al*: **Comparative secretome analysis of *Magnaporthe oryzae* identified proteins involved in virulence and cell wall integrity**. *Genom Proteom Bioinf* 2022, **20**(4):728-746.

35. Lee C-H, Liu Y-C, Chen C-J: **Development of a high-throughput kinase activity platform using nanoLC-MS/MS with DIA approach for studying the anti-cancer mechanism of Taxol in ovarian cancer**. *Analytica Chimica Acta* 2024, **1318**:342944.

36. Lou R, Shui W: **Acquisition and analysis of DIA-based proteomic data: A comprehensive survey in 2023**. *Mol Cell Proteomics* 2024, **23**(2):100712.

ARTICLE IN PRESS

37. Bersching K, Michna T, Tenzer S, Jacob S: **Data-Independent Acquisition (DIA) Is Superior for High Precision Phospho-Peptide Quantification in Magnaporthe oryzae**. *Journal of Fungi* 2023, **9**(1):63.

38. Ingebritsen TS, Cohen P: **Protein Phosphatases: Properties and Role in Cellular Regulation**. *Science* 1983, **221**(4608):331-338.

39. Bauer NC, Doetsch PW, Corbett AH: **Mechanisms Regulating Protein Localization**. *Traffic* 2015, **16**(10):1039-1061.

40. Chou KC, Shen HB: **Cell-PLoc: a package of Web servers for predicting subcellular localization of proteins in various organisms**. *Nat Protoc* 2008, **3**(2):153-162.

41. Chen M, Zhang W, Gou Y, Xu D, Wei Y, Liu D, Han C, Huang X, Li C, Ning W *et al*: **GPS 6.0: an updated server for prediction of kinase-specific phosphorylation sites in proteins**. *Nucleic Acids Res* 2023, **51**(W1):W243-w250.

42. Wagih O, Sugiyama N, Ishihama Y, Beltrao P: **Uncovering Phosphorylation-Based Specificities through Functional Interaction Networks***. *Molecular & Cellular Proteomics* 2016, **15**(1):236-245.

43. Bajracharya A, Dickey B, Qiu Y: **GST Pull-Down Assay to Study PIF4 Binding In Vitro**. *Methods Mol Biol* 2024, **2795**:195-212.

44. Khondker S, Han GS, Carman GM: **Phosphorylation-mediated regulation of the Nem1-Spo7/Pah1 phosphatase cascade in yeast lipid synthesis**. *Adv Biol Regul* 2022, **84**:100889.

ARTICLE IN PRESS

ARTICLE IN PRESS

45. Anche V, Fakas S: **Complementation studies of the Pah1-encoded phosphatidate phosphatase in *Yarrowia lipolytica***. *The FASEB Journal* 2021, **35**(S1).

46. Liu N, Yun Y, Yin Y, Hahn M, Ma Z, Chen Y: **Lipid droplet biogenesis regulated by the FgNem1/Spo7-FgPah1 phosphatase cascade plays critical roles in fungal development and virulence in *Fusarium graminearum***. *New Phytol* 2019, **223**:412-429.

47. Zaremberg V, McMaster CR: **Differential partitioning of lipids metabolized by separate yeast glycerol-3-phosphate acyltransferases reveals that phospholipase D generation of phosphatidic acid mediates sensitivity to choline-containing lysolipids and drugs**. *J Biol Chem* 2002, **277**(41):39035-39044.

48. Guan B, Yu-Tong J, De-Li L, Wen-Hui L, and Xue H-W: **Phosphatidic acid suppresses autophagy through competitive inhibition by binding GAPC (glyceraldehyde-3-phosphate dehydrogenase) and PGK (phosphoglycerate kinase) proteins**. *Autophagy* 2022, **18**(11):2656-2670.

49. Jiang C, Zhang X, Liu H, Xu JR: **Mitogen-activated protein kinase signaling in plant pathogenic fungi**. *PLoS Pathog* 2018, **14**(3):e1006875.

50. Xu JR, Staiger CJ, Hamer JE: **Inactivation of the mitogen-activated protein kinase Mps1 from the rice blast fungus prevents penetration of host cells but allows activation of plant defense responses**. *Proc Natl Acad Sci U S A* 1998, **95**(21):12713-12718.

ARTICLE IN PRESS

ARTICLE IN PRESS

51. Xu JR, Hamer JE: **MAP kinase and cAMP signaling regulate infection structure formation and pathogenic growth in the rice blast fungus Magnaporthe grisea**. *Genes Dev* 1996, **10**(21):2696-2706.

52. Zhang X, Bian Z, Xu JR: **Assays for MAP Kinase Activation in Magnaporthe oryzae and Other Plant Pathogenic Fungi**. *Methods Mol Biol* 2018, **1848**:93-101.

53. Liu X, Zhou Q, Guo Z, Liu P, Shen L, Chai N, Qian B, Cai Y, Wang W, Yin Z *et al*: **A self-balancing circuit centered on MoOsm1 kinase governs adaptive responses to host-derived ROS in Magnaporthe oryzae**. *Elife* 2020, **9**.

54. Cruz-Mireles N, Osés-Ruiz M, Derbyshire P, Jégousse C, Ryder LS, Bautista MJA, Eseola A, Sklenar J, Tang B, Yan X *et al*: **The phosphorylation landscape of infection-related development by the rice blast fungus**. *Cell* 2024, **187**(10):2557-2573.e2518.

ARTICLE IN PRESS

ARTICLE IN PRESS

Figure

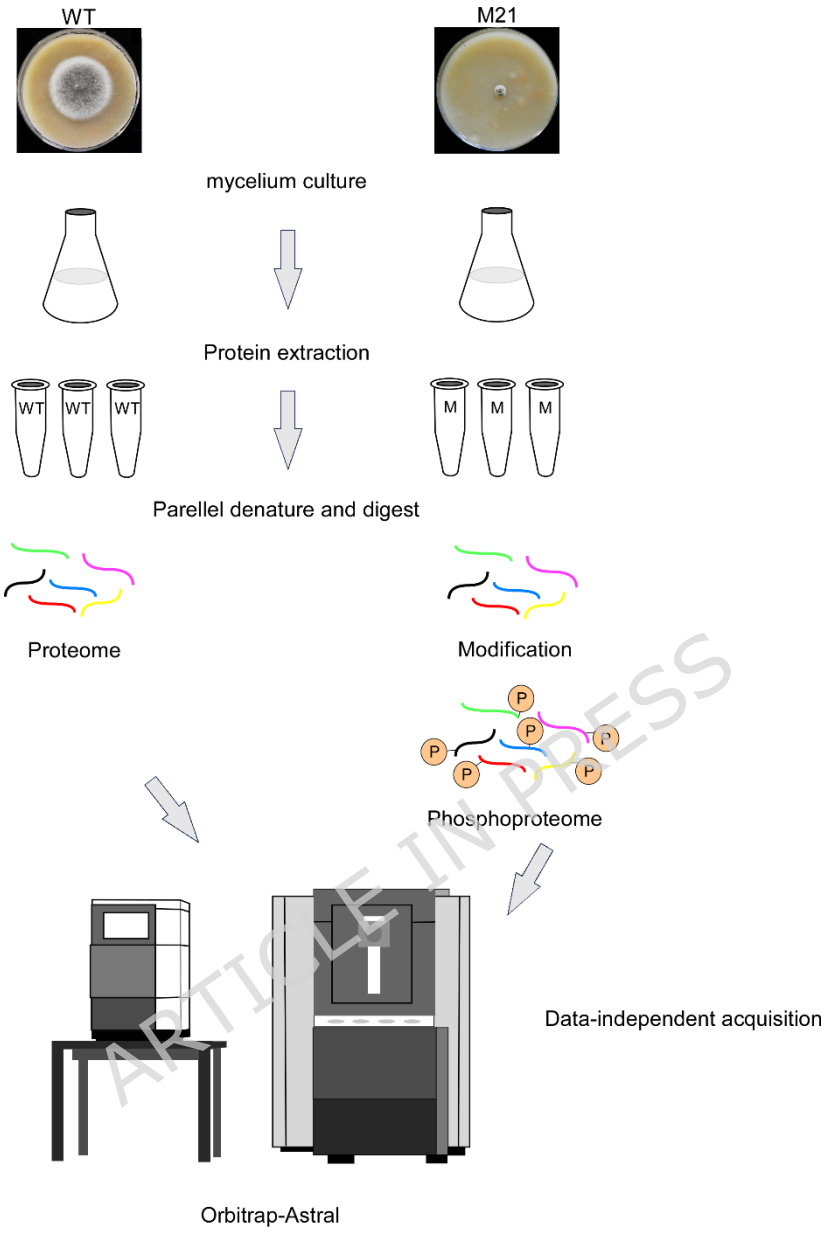


Figure 1. Schematic representation of the experimental workflow. The wild-type strain P131 (WT) and the MoPah1 deletion mutant (M21) of *Magnaporthe oryzae* were cultured in liquid minimal medium at 28°C with shaking at 120 rpm for 4 days. Mycelia were harvested from three independent biological replicates. Protein samples were denatured and digested in parallel for proteome analysis, whereas phosphoproteome samples underwent additional modification with trypsin treatment. All protein samples were analyzed using a quantitative data-independent acquisition

ARTICLE IN PRESS

approach on the Orbitrap Astral instrument.

ARTICLE IN PRESS

ARTICLE IN PRESS

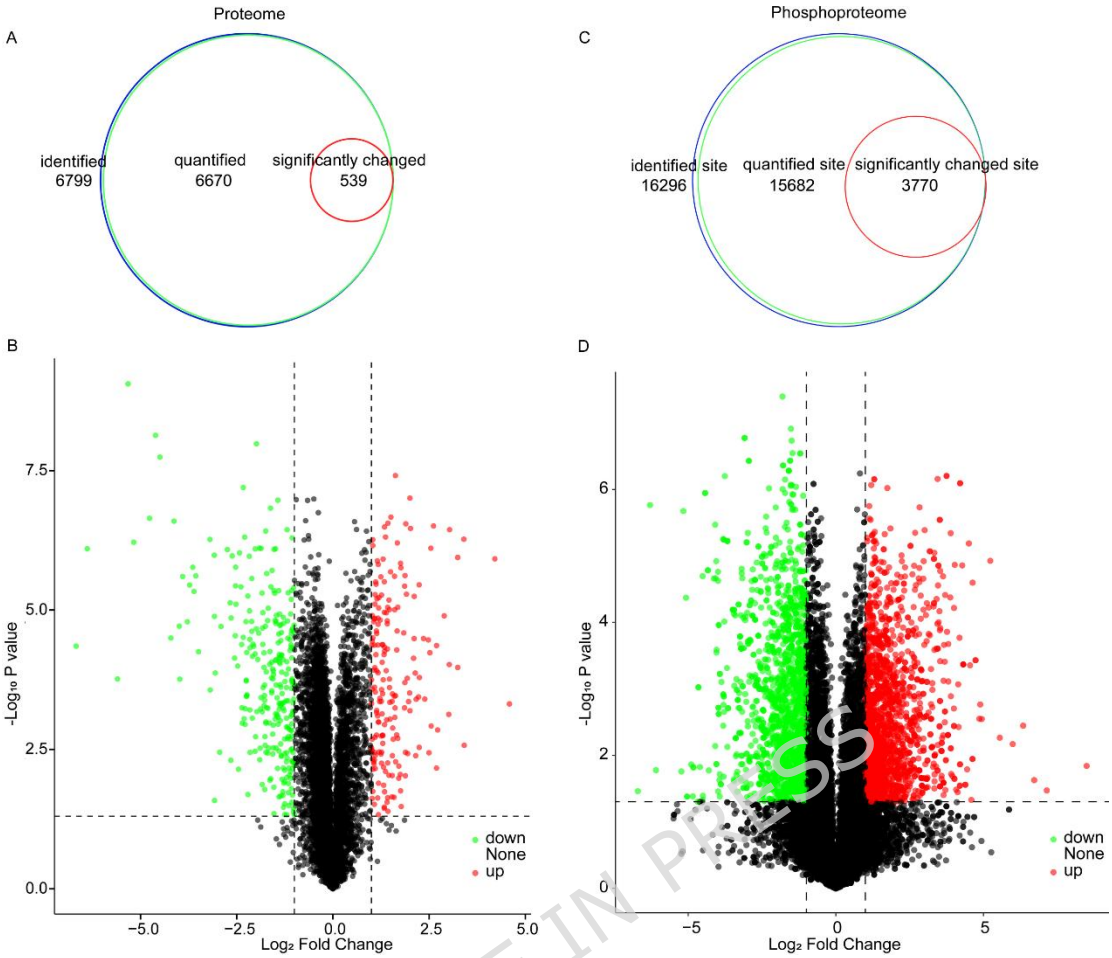


Figure 2. Identification and analysis of significantly differentially abundant proteins and phosphorylation sites. A. Overview of total proteins in the proteome. Blue cycle: 6,799 proteins identified in the proteome; green cycle: 6,670 proteins with intensity values greater than zero; red cycle: 539 proteins with significant changes in abundance in the M21. Proteins with a fold change >2.0 or <0.5 and an adjusted P value <0.05 were considered differentially abundant proteins. **B. Volcano plot showing upregulated and downregulated proteins in the mutant.** Green points: abundance decreased; red points: abundance increased; black points: no significant change. X-axis represents the Log2 fold change (M21/WT); Y-axis represents the negative Log10 of the P value from an independent *t*-test. **C. Overview of total phosphorylation sites identified in the phosphoproteome.** Blue cycle: 16,296 phosphorylation sites identified in the phosphoproteome; green cycle: 15,682

ARTICLE IN PRESS

phosphorylation sites with intensity values greater than zero; red cycle: 3,770 phosphorylation sites with significant changes in phosphorylation levels in the M21. Phosphorylation sites with a fold change >2.0 or <0.5 and an adjusted P value <0.05 were considered differentially abundant phosphoproteins. **D. Volcano plot showing upregulated and downregulated phosphorylation sites in the mutant.** Green points: decreased phosphorylation; red points: increased phosphorylation; black points: no significant change. The X-axis and Y-axis are the same as those shown in **B**.

ARTICLE IN PRESS

ARTICLE IN PRESS

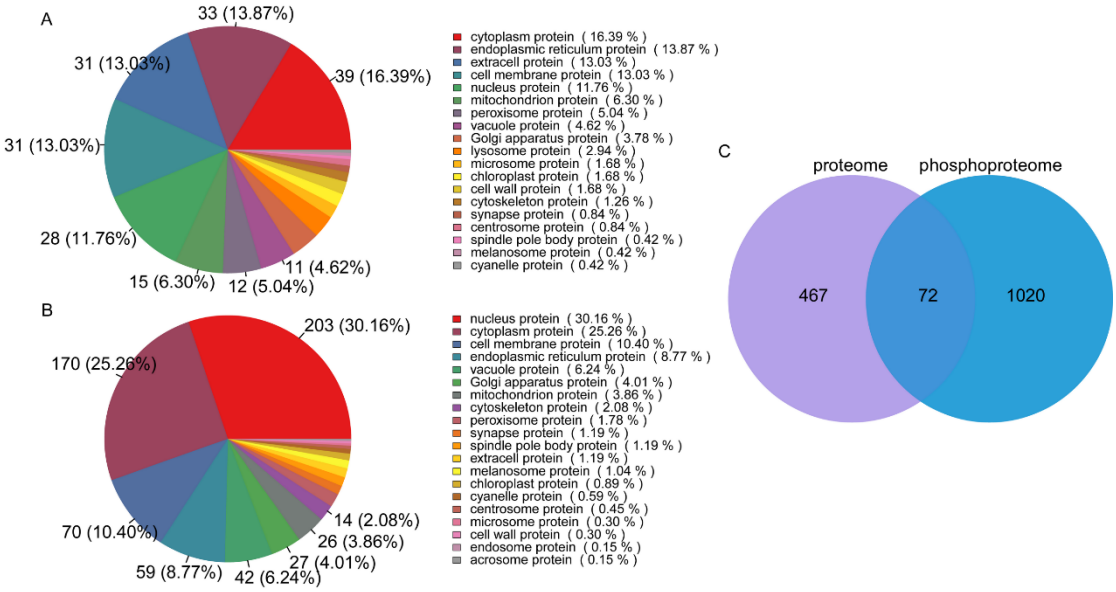


Figure 3. Subcellular localization prediction and overlap of significantly differentially abundant proteins and phosphoproteins. A. Predicted subcellular localization of DAPs. Different colored segments indicate the proportion of proteins localized to various subcellular compartments. **B. Predicted subcellular localization of DAPs and DAPPs.** Different colored segments indicate the proportion of proteins localized to various subcellular compartments. **C. Venn diagram showing the overlap between significantly altered proteins in the proteome and phosphoproteome.** Proteins with concurrent changes in both datasets are highlighted.

ARTICLE IN PRESS

ARTICLE IN PRESS

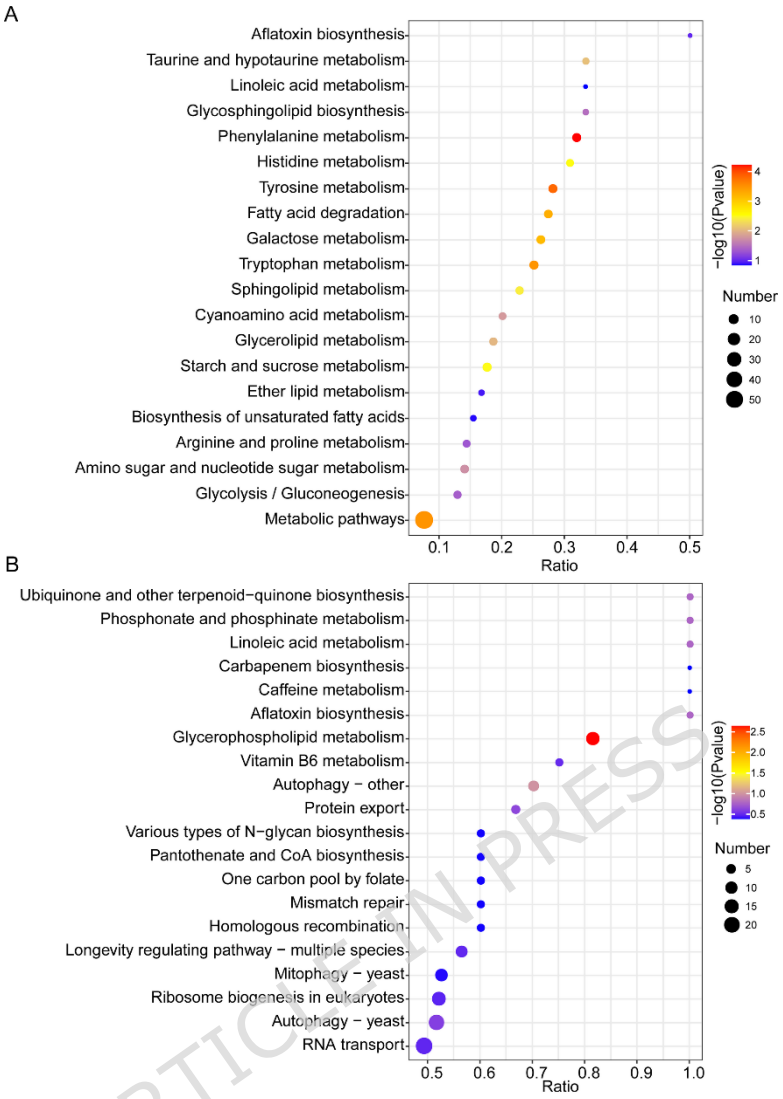


Figure 4. Functional enrichment analysis of DAPs and DAPPs. A, B. GO term enrichment for DAPs (A) and DAPPs (B).

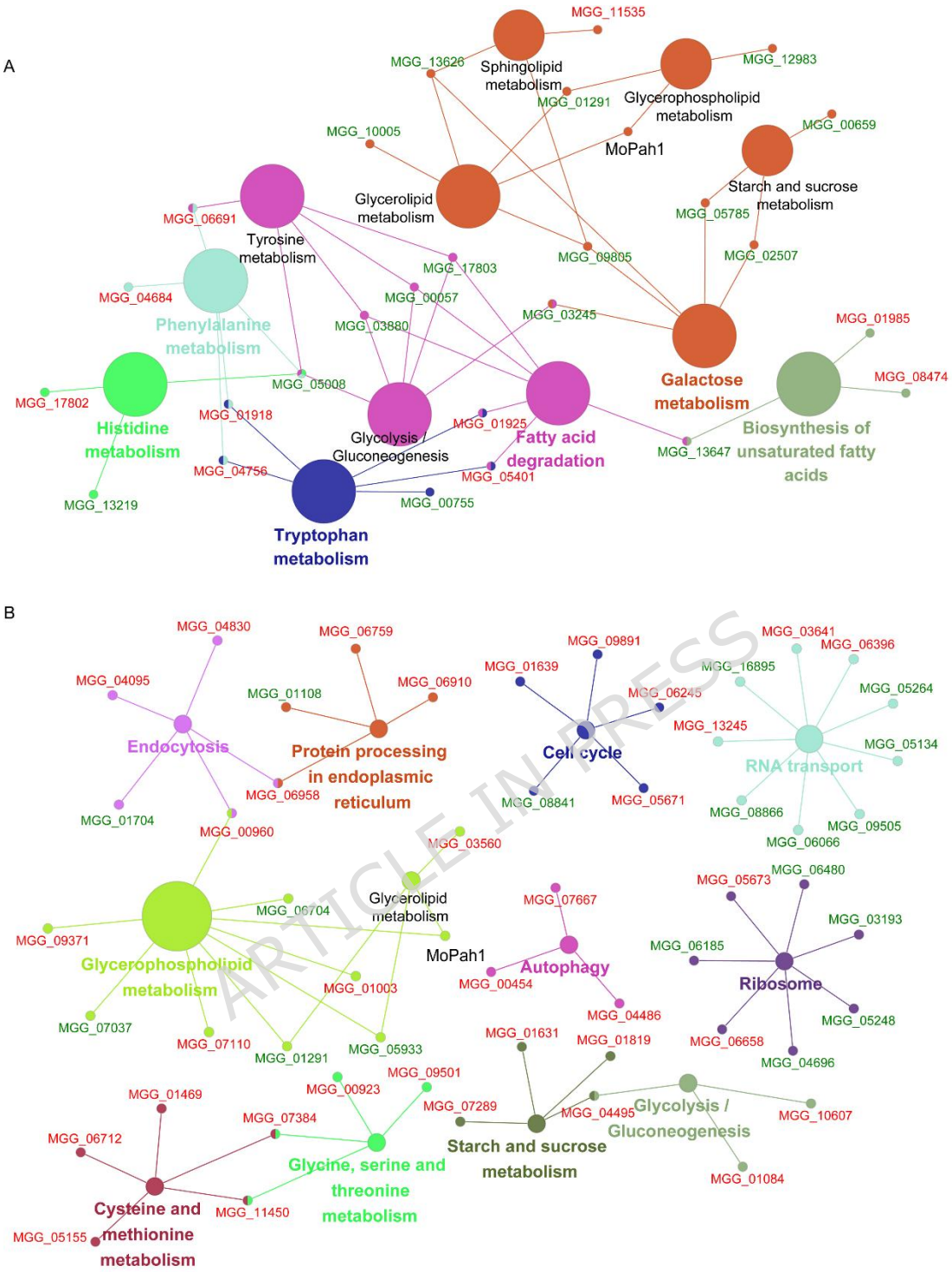


Figure 5. Protein interaction networks of differentially abundant proteins and phosphoproteins. A, B. STRING-based interaction networks of differentially abundant proteins (A) and phosphoproteins (B) in the mutant. Nodes represent enriched functional pathways, with confidence scores ranging from 0.9 to 1.0. Nodes representing pathways with no significant connections (≥0.9) are not shown. Red

ARTICLE IN PRESS

nodes: upregulated proteins and phosphorylation sites; green: downregulated proteins and phosphorylation sites.

ARTICLE IN PRESS

ARTICLE IN PRESS

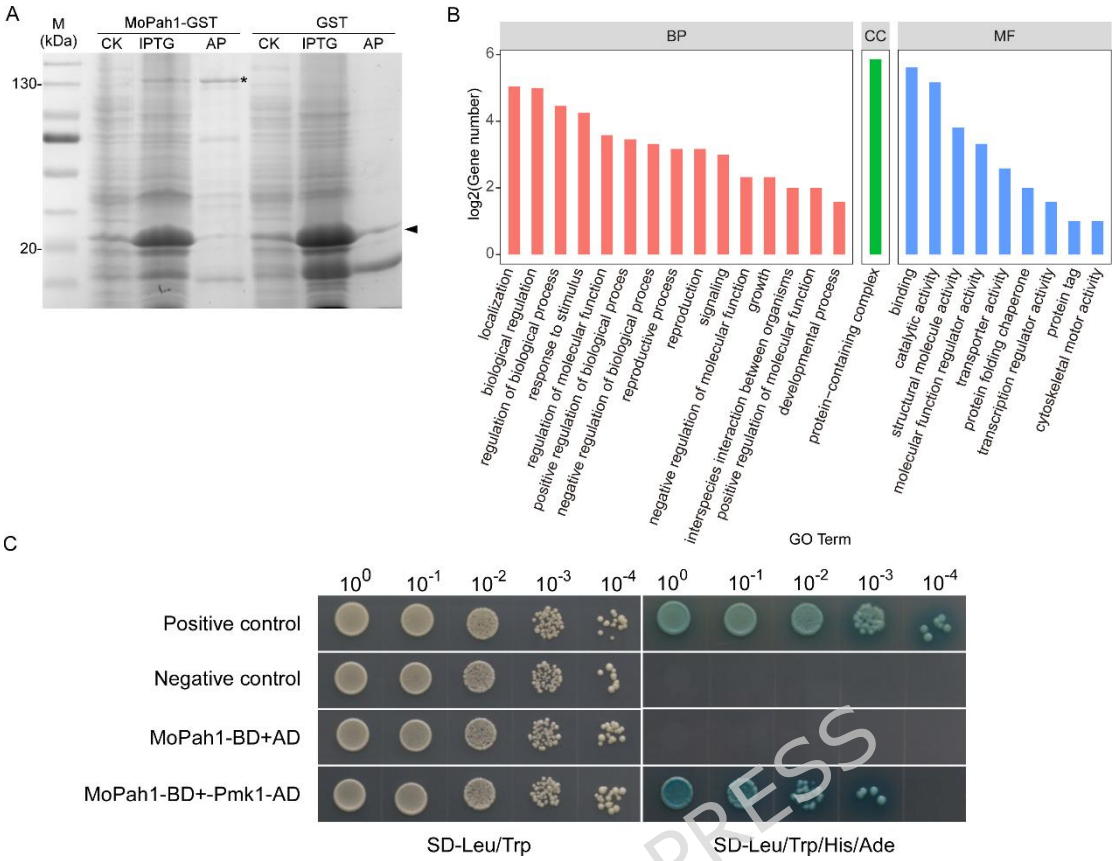


Figure 6. Identification and analysis of MoPah1 interactions. A. Affinity purification of MoPah1-GST protein in *E. coli*. Asterisks and arrows indicate the MoPah1-GST protein and GST tag, respectively. IPTG, isopropyl β-D-thiogalactoside. AP indicates affinity-purified proteins. **B. GO enrichment analysis of proteins interacting with MoPah1, identified via a GST pull-down assay. C. Yeast two-hybrid assay validating the interaction between MoPah1 and Pmk1 in *M. oryzae*.** SD-Leu/Trp and SD-Leu/Trp/His/Ade were used for the selective growth of AH109 transformants. BP: biological process; CC: cellular component; MF: molecular function.